

An Efficient ROI Encoding Based on LSK and Fractal Image Compression

TMP Rajkumar¹ and Mrityunjaya Latte²

¹Research Scholar, Anjuman Engineering College, India

²Principal, JSS Academy of Technical Education, India

Abstract: Telemedicine is one of the emerging fields in medicine which is characterized by transmitting medical data and images between different users. The medical images which are transmitted over the internet require huge bandwidth. Even images of single patient are found to be very huge in size due to resolution factor and number of images per diagnosis. So, there is an immense need for efficient compression techniques that can be used to compress these medical images. In medical images, only some of the regions are considered to be more important than the others (e.g., tumor in brain Magnetic Resonance Imaging (MRI)). This paper reviews the application of ROI coding in the field of telemedicine. The image coding is done using Wavelet Transform (WT) based on Listless Speck (LSK). The Region of Interest (ROI) is obtained from user interaction and coded with the user given resolution to get high Compression Ratio (CR). In our proposed method, instead of decompressing all the blocks, we decompress only the similar blocks based on the index valued stored on the stack. Thus, our proposed method efficiently compresses the medical image. The performance measure can be analyzed by using Peak Signal to Noise Ratio (PSNR). The execution time of the proposed method will be reduced when compare to the other existing methods. The experimental result shows that the application of ROI coding using LSK brings about high compression rate and quality ROI.

Keywords: Image compression, ROI, LSK, fractal image compression, MRI images, iterated functions systems.

Received January 28, 2012; accepted August 26, 2012; published online June 26, 2014

1. Introduction

Visual communication is becoming increasingly important with applications in several areas such as multimedia, communication, transmission and storage of remote sensing images, education and business documents and medical images etc., [18]. In many situations multiple, large images require processing in a short period of time [36]. Compression is useful because it helps reduce the consumption of expensive resources, such as hard disk space or transmission bandwidth [38]. Image compression is achieved by reducing redundancy between neighboring pixels but, preserving features such as edges and contours of the original image [29]. Increase in the use of color images in the continuous expansion of multimedia applications has increased the demand for efficient techniques that can store and transmit visual information. This demand has made image compression a vital factor and has increased the need for efficient algorithms that can result in high Compression Ratio (CR) with minimum loss [1]. There are various methods of compressing still images and every method has three basic steps: Transformation, quantization and encoding [19, 27].

Image compression may be lossy or lossless. Lossless compression is preferred for archival purposes and often for medical imaging, technical drawings, clip art, or comics. This is because lossy compression methods, especially when used at low bit rates, introduce compression artifacts. Various practical applications demands for high data rate compatibility

with a error tolerance and in such system lossy compression where more suitable. System where accuracy is prime factor lossy compression schemes cannot be used. To achieve higher compression with lower error modifier version of compression such as shape based compression is developed [28].

The compression of medical images has a great demand. The medical community has been very reluctant to adopt lossy algorithms in clinical practice. However, the diagnostic data produced by hospitals has geometrically increased and a compression technique is needed that results with greater data reductions and hence transmission speed. In these cases, a lossy compression method that preserves the diagnostic information is needed [35]. Medical images used at medical facilities are now commonly digitalized due to corresponding advances in information technology. Computed Tomography (CT) or Magnetic Resonance Image (MRI) generates digitalized signals by its own and diagnostic images from legacy devices can be digitalized by film scanner and such [20]. Lossless compression with progressive transmission is playing a key role in telemedicine applications [24, 25].

The lossy image compression techniques, which reproduce completely acceptable decoded images on scenes such as houses or landscapes, do not fulfill the strictest quality requirements needed in medical applications. There is always the possibility that a

vague detail might give a reason to suspect some critical changes in a patient's condition. For this reason, the lossy techniques, which tend to give high CRs, such as 1:10-1:30, are not acceptable in medical image compression [21]. Image compression is required to minimize the storage space and reduction of transmission cost. Medical images like MRI and CT are special images require lossless compression as a minor loss can cause adverse effects. Prediction is one of the techniques to achieve high compression. It means to estimate current data from already known data [26]. Image communication systems for medical images have bandwidth and image size constraints that result in time-consuming transmission of uncompressed raw image data. Thus, image compression is a key factor to improve transmission speed and storage, but it risks losing relevant medical information. It exploits common characteristics of most images that are the neighboring picture elements or pixels are highly correlated [1]. It means a typical still image contains a large amount of spatial redundancy in plain areas where adjacent pixels have almost the same values [15]. Medical imaging modalities include:

1. CT.
2. MRI.
3. Ultrasonography (US).
4. X Radiographs, etc.

These modalities provide flexible means for viewing anatomical cross sections and physiological states. Medical images are mostly gray scale images, with diagnostically important region in the middle of the image and background of the image is usually uniform dark gray [30]. The improved compression performance will be accomplished by making use of clinically relevant regions as defined by physicians. Images taken of patients will be aligned to pre-stored image models stored in an atlas. The atlas will contain models of typical classes of images. If we are trying to compress a chest x-ray image, then it will be matched with a pre-stored chest x-ray model that is stored in the atlas [8, 41].

High quality compression on cardiac MR images using wavelet-based methods has been compared with standard JPEG. Since, the last one is an unrestricted algorithms designed for true-color realistic images, its performance compressing gray level images can be improved with alternate algorithms specifically designed for this purpose [34]. Using image compression techniques, such as JPEG, can no doubt reduce the physical size of image but the image quality is unavoidable to degrade [1]. To obtain improved image quality, median filtering is applied as post-processing [22].

In our proposed method, the given medical image can be compressed using LSK encoder and to avoid compression on similar blocks of the image using fractal image compression. The self similarity of the

image blocks can be calculated using Euclidean distance. The rest of the paper is organized as follows: Section 2 describes some of the recent related works. Section 3 briefs the fractal image compression process. The proposed part is detailed in section 4. Experimental results and analysis of the proposed methodology are discussed in section 5. Finally, concluding remarks are provided in section 6.

2. Related Works

Numerous researches have been proposed by researchers for the medical image compression process. In this section, a brief review of some important contributions from the existing literature is presented.

Ganguly *et al.* [13] deals with the various aspects and types of medical imaging. With the growth of computers and image technology, medical imaging has greatly influenced the medical field. The diagnosis of a health problem was highly dependent on the quality and the credibility of the image analysis.

El-Rube *et al.* [11] proposed a contour let-based compression scheme for medical endoscope images. The proposed algorithm was compared with two well known transform coding algorithms; the Discrete Cosine Transforms (DCT) and the Wavelet Transform (WT).

Tamilarasi and Palanisamy [32] proposed a wavelet based contour let image compression algorithm. Recent reports on natural image compression have shown superior performance of contour let transform, a new extension to the WT in two dimensions using Laplacian Pyramid (LP) and directional filter banks. In the diagnosis of medical images, the significant part Region Of Interest (ROI) was separated out from the rest of the image using fuzzy C-means algorithm and then to the resultant image optimized contour let transform was applied to enhance the visual quality.

Bhat *et al.* [7] proposed a scheme allows achieving a CR up to approximately 40:1 with reasonable image quality.

Yang *et al.* [39] developed an information hiding methodology that includes the RSA encryption algorithm and a DCT based hiding technique. With that system, any medical image that would be electronically transferred (i.e., emailed, faxed, etc.) would have the patient's information hidden and embedded in the image outside of the ROI.

Sumalatha *et al.* [31] proposed a lossless compression approach based on 3D integer wavelet transform, 3D SPIHT algorithm of MR images. The use of lifting scheme allows to generate truly lossless integer to integer wavelet transforms. The main objective of that work was to reject the noisy background and reconstructs the image portion losslessly.

Bhardwaj and Ali [6] attempted to describe the algorithm for image compression using MFHWT and

showed better results than those obtained by using any other method on an average. It includes a number of examples of different images to validate the utility and significance of algorithm's performance.

Gaudeau and Moureaux [14] presented a new lossy coding scheme based on 3D WT and lattice vector quantization for volumetric medical images. The main contribution of that work was the design of a new codebook enclosing a multidimensional dead zone during the quantization step, which enables to better account correlations between neighbor vowels. Furthermore, they presented an efficient rate-distortion model to simplify the bit allocation procedure for our intra-band scheme. Their algorithm has been evaluated on several CT and MRI volumes.

3. Fractal Image Compression

The mathematical process called Fractal encoding is utilized to encode a given image into a set of mathematical data that illustrates the fractal properties of the image [16]. Fractal encoding is based on the fact that all objects consists of information in the form of related, repeating patterns called an attractor. An image is converted into fractal code mostly by fractal encoding. The huge number of iterations required to determine the fractal patterns in an image makes the encoding process to have extreme computation [9, 33]. Either Iterated Function Systems (IFS) or by Partitioned Iterated Function Systems (PIFS) are used to achieve FIC [37].

3.1. Iterated Functions Systems

Here, we briefly present the underlying mathematical principles of fractal image compression based on a theory of IFS [4, 12]. An IFS consists of a collection of contractive affine transformations $\{w_i: M \rightarrow M | 1 \leq i \leq m\}$, where w_i maps a metric space M to itself. A transform w is said to be contractive when there is a constant number $s(0 \leq s < 1)$ and $d(w(\mu_1), w(\mu_2)) \leq s d(\mu_1, \mu_2)$ hold for any points $\mu_1, \mu_2 \in M$, where $d(\mu_1, \mu_2)$ denotes the metric between μ_1 and μ_2 . The collection of transformations defines a map $W(S) = \bigcup_{i=1}^m w_i(S)$, where $S \subset M$. Note that, the map W is applied not to the set of points in M but to the set of sub-sets in M . Let W be a contractive map on a compact metric space of images with the bounded intensity and then the contractive mapping fixed-point theorem asserts that there is one special image x_w , called the attractor, with the following properties:

1. $W(x_w) = x_w$.
2. $x_w = \lim_{n \rightarrow \infty} W^n(S_0)$, which is independent of the choice of an initial image S_0 .

Fractal image compression relies on this theorem. Suppose the attractor of a contractive map W is the original image to be compressed. From property 2, the original image is obtained from any initial image by applying W . The goal of fractal image compression is to find the contractive map whose attractor is

sufficiently close to the original image and to store the parameters of W instead of the intensity values.

4. An Efficient Technique for Image Compression using LSK and Fractal Image Compression Method

Compressing the medical images effectively by employing, Listless Speck (LSK) and fractal image compression techniques. The primary intension of our research is to compress the medical image efficiently. So initially, the medical image is divided into number of equal sized blocks. In a medical image, more number of blocks is similar. In order to, avoid compression on all the similar blocks; the fractal image compression technique can be used. So, this fractal image compression technique will identify all the similar blocks in the image [3]. Then, store all the similar blocks and its indexes in the separate stack. Compress the image by employing LSK method. The entire process of the proposed method is described in the following.

Let us considered the set of medical images $D\{I_1, I_2, \dots, I_N\}$. Here I be the image of size $M \times N$. Then, divide the image into number of $P \times P$ non overlapping blocks. This can be represented as:

$$I = \{Ib_1, Ib_2, \dots, Ib_{nb}\} \tag{1}$$

Where, Nb represents the total number of blocks in the image. After the block division, the similar blocks in the image can be identified by employing the concept of fractal image compression scheme.

4.1. Fractal Image Compression

The property of self-similarity of fractal objects is used by fractal compression and fractal encoding [5, 17]. Some of the blocks obtained by dividing the color image into several 8×8 blocks are similar.

Our proposed method, calculates the similarity of the a^{th} block for the fractal image compression by comparing the distance measure of the a^{th} block and its n neighboring blocks. The following equation is used to calculate the distance measure:

$$S_d = \sqrt{\sum (Ib_a - Ib_b)^2} \tag{2}$$

Here, Ib_a and Ib_b ; where $b = \{1, 2, \dots, n\}$ represent the current block and blocks adjacent to the current block, respectively. This is shown in the following Figure 1.

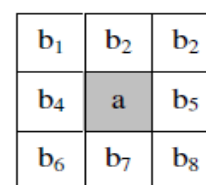


Figure 1. Range blocks and domain blocks.

The flag value is set according to the threshold D_{ish_2} after the distance measure is calculated. The calculated

distance S_d is compared with the threshold D_{ish} as follows:

$$I_F^b = \begin{cases} I_F^b = 1; & \text{if } S_d < D_{ish} \\ I_F^b = 0; & \text{otherwise} \end{cases} \quad (3)$$

Here, b and F represent the image block and the flag value of each block of the image, respectively. Both a^{th} and b^{th} blocks are said to be similar if the b^{th} block yields a flag value of 1, when it is compared with the a^{th} block. Otherwise, they are said to be dissimilar. This is illustrated in Figure 2:

1	1	0
1	a	0
1	0	0

Figure 2. Flags assigned to each domain blocks.

So, we store the indices by identifying the blocks similar to the a^{th} block. In fractal image compression, a^{th} block is the range block and the analogous similar blocks are domain blocks. Instead of all the similar domain blocks, we use only the range block once the indices of range block and its corresponding domain blocks are accumulated. The time and memory complexity is decreased by this.

After identifying the similar blocks in an image using Fractal image compression technique the similar blocks and its corresponding indexes are stored in the separate stack for decompression process. These similar blocks are then compressed by using LSK encoder.

4.2. Listless Speck

LSK [10] represents Listless set partitioning embedded block. Same block partitioning rules used by Speck are also used by LSK. By placing markers at all initial pixels for all the sub-bands, partitioning of set ‘P’ into three ‘S’ sets is modified in the proposed algorithm [29]. Though the proposed LSK algorithm employs some minimum number of bits to specify the insignificant sub-band blocks in the initial passes, the required computational time and complexity are similar to that of speck [7].

This paper describes a new image/video codec called LSK that uses the set partitioning rules of speck and does an explicit breadth first search without using lists. State information is kept in a fixed size array that corresponds to the array of coefficient values; with about four bits per coefficient to enable fast scanning of the bit planes.

4.2.1. Storage

In the DC band, the number of coefficients is determined as:

$I_{dc} = R_{dc} C_{dc}$, where, $R_{dc} = R2^{-L}$, $C_{dc} = C2^{-L}$, L is the number of sub-band decomposition levels. A vector of length I

is used to store these coefficients. For ease, array val and array $sign$ are used to refer to the magnitude part and the sign part respectively. An array, named $mark$, of length I , each coefficient consisting of 2 bits represents the state table. A one-to-one correspondence exists between val and $mark$.

For LSK, the pre-computed maximum descendent magnitude array, $d\ max$, has length $I/14$ and the maximum grand descendant magnitude array, $g\ max$, has length $I/16$. These arrays can be eliminated at the expense of repeated searching over significant trees for significant coefficients at the encoder.

4.2.2. State Table Markers

In order to, keep track of the set partitions, the following markers are kept in the 2 bit per coefficient state table $mark$. Each element of mark indicates something about the corresponding element in the val image array, if it signifies a block. Each marker and its meaning are listed below:

- *MIP*: The pixel is unimportant or untested for this bit-plane.
- *MNP*: The pixel is newly important, so it will not be refined for this bit-plane.
- *MSP*: The pixel is important and will be refined in this bit plane.
- *MS2*: The block is of size 2×2 , i.e., 4 elements to be skipped.

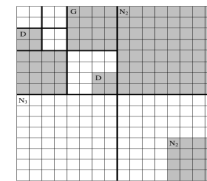


Figure 3. State array diagram of LSK.

In Figure 3, *MD* stands for marker *D*. The *MD* is the first child pixel of each descendent set and *MG* is the pixel of the first grandchild in a set consisting of all grand descendants of its grandparent pixel, but not including the grand parent or the children of the grand parent. *MN* is the first grandchild of *MD* set. *MN₃* is a first great grandchild of *MD* or *MG*. Lower levels of the set are labeled with *MN₂* markers.

4.2.3. Initialization

Floating point transform coefficients are quantized to integers by performing a dyadic sub band transform on the image, with $L = 5$ levels. After that, the transform is read into the linear array val . The entire two-dimensional transform matrix is mapped into one-dimensional array and it can be found for each (r, c) by bit interleaving and the corresponding coefficients can be moved. val is scanned to find the most important non zero bit plane, B .

In LSK, this procedure can be included by employing additional pointer in the proposed algorithm, to skip all the elements after it. Each coefficient is marked with *MIP* and first element of

every full sized block with MS^* markers to initialize the state table.

$$mark[i] = MIP \quad (4)$$

$$mark[i + j] = MS2 \quad (5)$$

Where, $j=0, 1, 2, \dots, e$ and $e = \log_2(m/2^l)$. During initialization, some full sized blocks are marked. To avoid computing the above indices, a small pre-computed constant look up table can be used.

4.2.4. Encoder Algorithm

The main encoder algorithm performed for each bit-plane, b , starting with B and decremented to 0, or until a bit budget is met. There are three passes in the algorithm. They are:

1. Insignificant Pixel Pass.
2. Insignificant Set Pass.
3. Refinement Pass. For each Bit-plane, the Significance Level is given by. $s=2^b$.

In binary form, s has a single bit set, at a bit position b , the test to determine whether the coefficient $val[i]$ is newly significant is $d=val[i]$ and s . The coefficient is newly significant if and only if its b^{th} bit is set. If d is non zero, $val[i]$ significant. Start with Insignificant pixel pass, the new significant elements are identified and marked as the MNP . Then, move to next element. This can be described as if $mark[i]=MIP$ then the elements in the state array are marked as MNP i.e.

$$output(d = S_b[val(i)]) \quad (6)$$

$$mark[i]=MNP \quad (7)$$

Then, start the Insignificant Set pass, the block significance can be checked in the state table $mark$. If the block is significant means it is split up into 4 children. Then, check the block significance of the children. If the grand descendent block is significant we can further divide them into four. And check for the significance once again. This can be described by the following pseudo code:

For each j in n

$mark[i+j*2^{(cnt-MS2-1)} \text{ to } i+j*2^{(cnt-MS2-1)} + cnt-MS2-1]=MS2$

End for

In the refinement pass, set $mark[i]=MSP$ and $i=i+2^{cnt-ms2}$. The same procedure followed by the encoder is also followed by the decoder but with a few low level changes.

The main reason for the increase in memory requirement is because of this use of the state table markers. LSK uses linear indexing technique and utilizes coefficients stored in a linear array for the coding process unlike SPIHT, Speck and other existing algorithms which operate on a two dimensional array of coefficients. In addition to, simplifying the parent-child relationship in Hierarchical Trees, skipping of child trees has also been made easy by such use of linear array [39, 40]. Therefore, the complexity of the algorithm is less compared to other existing

algorithms. Figure 4 illustrates the entire compression process.

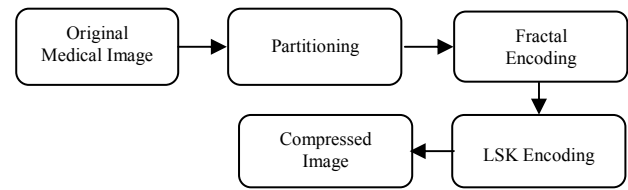


Figure 4. Block diagram of the compression process.

4.3. Decompression Process

The decompression process is quite simple. We first decode the fractal parameters and repeatedly transform an arbitrary image by fractals.

A fractal approximation of the original image is produced by this process. Finally, we get the decompressed image by transforming the addition of the fractal approximation and the difference image by LSK decoding. Figure 5 illustrates the entire decompression process.

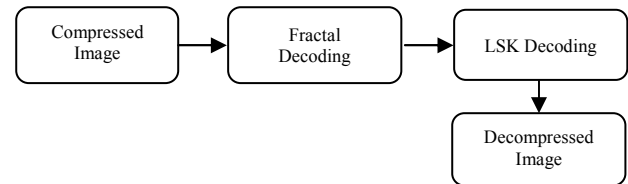


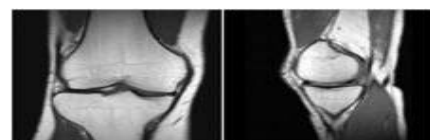
Figure 5. Block diagram of the decompression process.

5. Experimental Results

In this section, we illustrate the effectiveness of the proposed image compression scheme by means of the results obtained from the experimentation. The proposed method was implemented in MATLAB (Mat lab 7.10) and the proposed compression scheme was evaluated using medical images. The test images used in the experiments include: Knee MRI and Brian MRI images [10]. The sample output obtained from the proposed method is as follows:

Initially, after input the image from the database, select the region of interest in the input image. This can be represented in Figures 6 and 7. Both knee and brain MRI images are used for compression process. This figure also shows the selected region from the image. Then, block partitioning process is performed. The selected region from the input image is divided into blocks of same size. This can be described in Figure 8.

Figures 9 and 10 represent the decompression process of the ROI selected portion of the input image. The original image compression without ROI selection is displayed in Figures 11 and 12.



a) Original image.

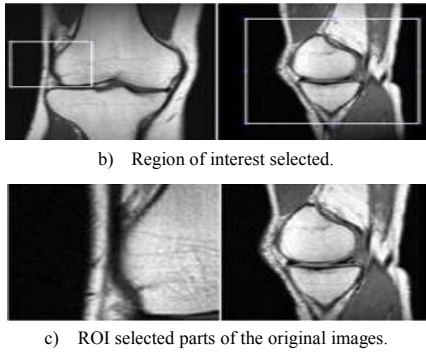


Figure 6. The sample output obtained from the ROI selection process in Knee MRI images.

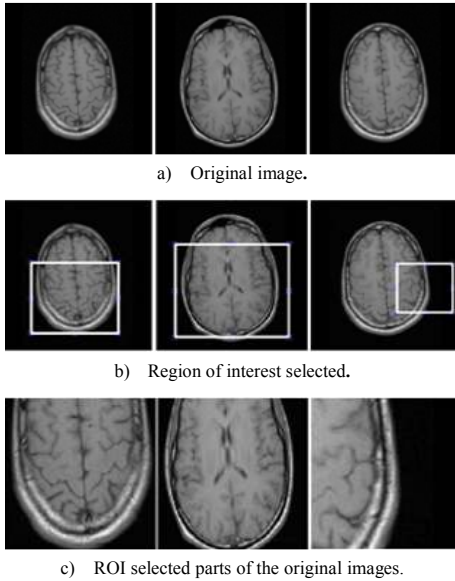


Figure 7. The sample output obtained from the ROI selection process in brain MRI images.

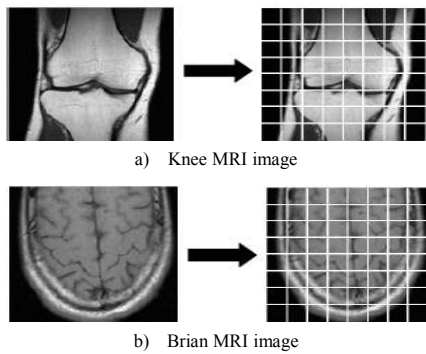


Figure 8. The sample output obtained from the block partitioning process.

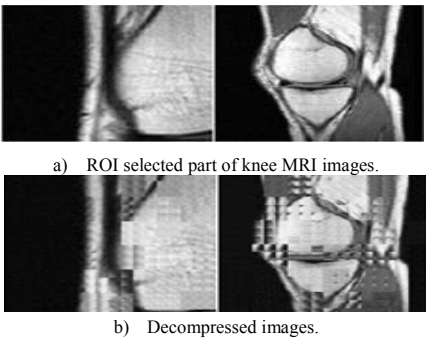


Figure 9. The sample output obtained from the proposed compression process.

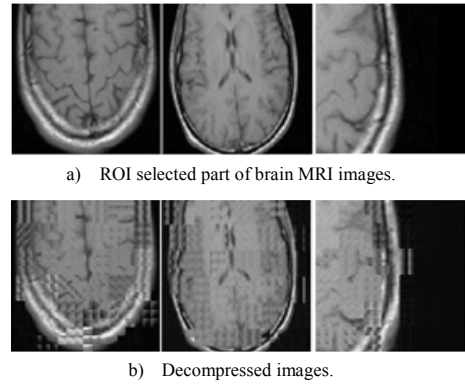


Figure 10. The sample output obtained from the proposed compression process.

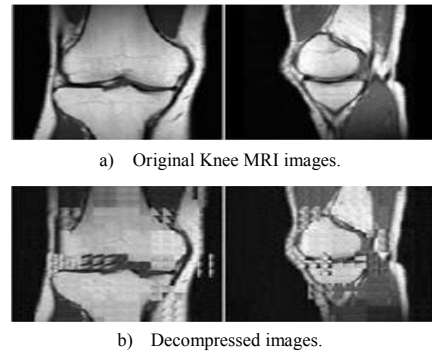


Figure 11. The sample output obtained from the compression process without ROI selection.

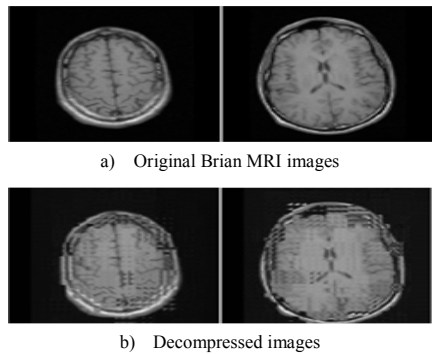


Figure 12. The sample output obtained from the compression process without ROI selection.

Comparative Analysis: In the comparative analysis part, the proposed method is compared with the existing image compression process in terms of Peak Signal to Noise Ratio (PSNR) measures.

PSNR: To evaluate the performance of the motion estimation technique in the proposed system, the PSNR based on the Mean Square Error (MSE) is used as a quality measure and its value can be determined using the following equation:

$$PSNR = 10 \log \left(\frac{(255)^2}{MSE} \right) dB \quad (8)$$

$$MSE = \frac{1}{MN} \sum (\hat{f}(x, y) - f(x, y))^2 \quad (9)$$

Here, MN is the total number of pixels in the image. $\hat{f}(x, y)$ is the decompressed image and $f(x, y)$ is the original image. Initially, we compare the PSNR values

for the proposed compression scheme with ROI selection and without ROI selection. For our proposed method, we use both Knee and Brian MRI images. The Figures 13 and 14 show the comparison of the proposed method with ROI selection and without ROI selection.

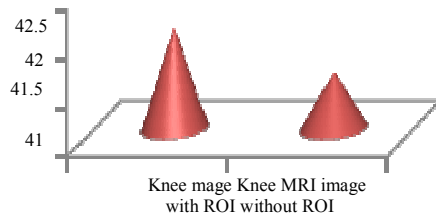


Figure 13. PSNR comparison of the proposed method with and without ROI selection process in Knee MRI images.

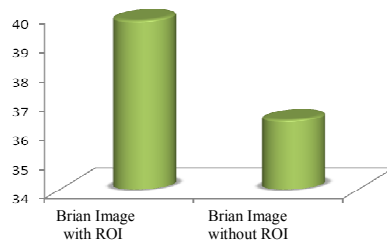


Figure 14. PSNR comparison of the proposed method with and without ROI selection process in Brian MRI images.

From the Figures 13 and 14, we observe that the proposed method gives high PSNR values in ROI selection method. These details can be described in Table 1.

Table 1. PSNR comparisons of proposed method.

Methods	PSNR (in dB)	
	Knee MRI	Brian MRI
Proposed Method with ROI Election	42.0396	39.79625
Proposed Method without ROI Election	41.5789	36.3733

Then, we compared the proposed method with other existing methods. The Table 2 represents the PSNR values of the proposed method and the other existing methods.

Table 2. The PSNR comparison between proposed and existing methods.

Methods	PSNR (in dB)
Two Component Compression Method	37.91
modified EZW	32.08
ROI with EZW	36.1
Proposed Method	40.91
SOFM	27.7
MFHWT	27.1348

The image quality of the decompressed image is better when compared to the existing methods. So that, the proposed methodology obtained better PSNR values. In our proposed method the image quality and CR can be improved based on the LSK encoder and similar block identification process.

From Table 2, we observed that the proposed method has the better PSNR values when compared to the existing methods such as two component compression method [35], Modified EZW [32], ROI

with EZW [2] SOFM [7] and MFHWT [6]. This can be described in Figure 15.

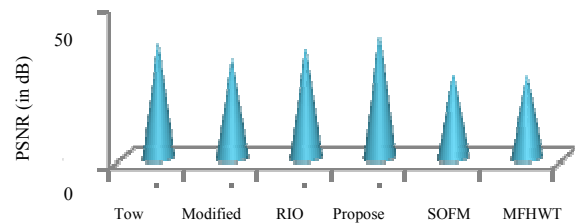


Figure 15. PSNR comparison.

CR: Is the ratio between the number of bits required storing the image before compression I and the number of bits required to store the image after compression O .

$$CR = I/O \tag{10}$$

Here, I is the size of the original image and O is the size of the decompressed image. The following table describes the CR for the proposed method. Here, we observe that the proposed method with ROI selection process is highly compressed when compared to the proposed method without ROI selection process.

Table 3. The CR comparison of the proposed method.

Methods	CR	
	Knee MRI	Brian MRI
Proposed Method with ROI Selection	2.80:1	3.435:1
Proposed Method without ROI Selection	3.014:1	4.88:1

Figure 16 represents the CR of the both knee and brian MRI images in proposed method. From this results, we conclude that our proposed method with ROI selection process gives high PSNR values and efficient CR when compared to the other existing methods.

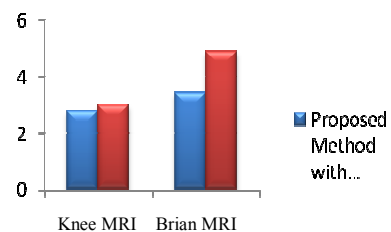


Figure 16. CR comparison.

6. Conclusions

The application of ROI coding in the field of telemedicine has been presented in this paper. An efficient compression scheme with fractal encoding has been proposed in this article. The proposed encoding scheme made use of the renowned wavelet based image encoding scheme LSK. The ROI coding begins with the selection of ROI by the user. By employing the fractal encoding, we identify the similar blocks in the given input image. By using LSK encoder, the different ROIs are encoded. The final encoded data is formed by integrating all the encoded ROI image data, and the similar, dissimilar blocks with its indexes. In

the decoder, each ROI is decoded using the encoded data and the information available in the header. Using the co-ordinate details in the header the decoded ROI image data are placed in their corresponding results. The experimental results show that the proposed encoding scheme using LSK gives high CR and better PSNR values.

References

- [1] Annadurai S. and Sundaresan M., "Wavelet Based Color Image Compression using Vector Quantization and Morphology," in *Proceedings of International Conference on Advances in Computing, Communication and Control*, New York, USA pp. 391-396, 2009.
- [2] Babu D. and Alamelu N., "Wavelet Based Medical Image Compression using ROI EZW," *International Journal of Recent Trends in Engineering*, vol. 1, no. 3, pp. 97-100, 2009.
- [3] Balraju M., Govardhan A., Chandra N., Basha S., and Srinivas P., "Loss Controllable Image Compression for Color Images using Block Based Binary Plane Technique," *International Journal of Engineering Studies*, vol. 1, no. 1, pp. 59-70, 2009.
- [4] Barnsley M., *Fractals Everywhere*, Second Edition, Elsevier, 1993.
- [5] Barnsley M., Ervin V., Hardin D., and Lancaster J., "Solution of an Inverse Problem for Fractals and Other Sets," *National Academy of Sciences of the United States of America*, vol. 83, no. 7, pp. 1975-1977, 1986.
- [6] Bhardwaj A. and Ali R., "Image Compression using Modified Fast Haar Wavelet Transform," *World Applied Sciences Journal, World Applied Sciences Journal*, vol. 7, no. 5, pp. 647-653, 2009.
- [7] Bhat G., Baba A., Khan E., "Efficient Image Compression Technique using Self Organizing Feature Maps," *International Journal of Engineering Science and Technology*, vol. 2, no. 12, pp. 7609-7615, 2010.
- [8] Bhavani S., "Performance Evaluation of Adaptive Mesh Based 3D MRI Compression using Wavelet Coding Schemes," *International Journal of Engineering Science and Technology*, vol. 2, no 6, pp. 2354-2358, 2010.
- [9] Bovik Z. and Alan C., "A Universal Image Quality Index," *IEEE Signal Processing Letters*, vol. 9, no. 3, pp. 81-84, 2002.
- [10] Brian MRI images from <http://brainweb.bic.mni.mcgill.ca/brainweb/>.
- [11] El-Rube I., Fayed H., and El-Nahas S., "Medical Endoscopic Image Coding: A Comparative Study," *Canadian Journal on Image Processing and Computer Vision*, vol. 1, no. 2, pp. 16-21, 2010.
- [12] Fisher Y., *Fractal Image Compression*, Springer, New York, 1995.
- [13] Ganguly D., Chakraborty S., and Kim T., "A Cognitive Study on Medical Imaging," *International Journal of Bio-Science and Bio-Technology*, vol. 2, no. 3, pp. 1-18, 2010.
- [14] Gaudeau Y. and Moureaux J., "Lossy Compression of Volumetric Medical Images with 3D Dead-zone Lattice Vector Quantization," *Annals of Telecommunications*, vol. 64, no. 5-6, pp. 359-367, 2010.
- [15] Ghrare S., Ali M., Jumari K., and Ismail M., "An Efficient Low Complexity Lossless Coding Algorithm for Medical Images," *American Journal of Applied Sciences*, vol. 6, no. 8, pp. 1502-1508, 2009.
- [16] Gray R. and Neuhoff D., "Quantization," *IEEE Transaction Information Theory*, vol. 44, no. 6, 1998.
- [17] Jacquin A., "Fractal Image Coding: A Review," in *Proceedings of IEEE*, pp. 1451-1465, 1993.
- [18] Kharate G, Ghatol A., and Rege P., "Image Compression using Wavelet Packet Tree," *ICGST-GVIP Journal*, vol. 5, no. 7, pp. 41-43, 2005.
- [19] Kharate G. and Patil V., "Color Image Compression Based On Wavelet Packet Best Tree," *International Journal of Computer Science Issues*, vol. 7, no. 2, pp. 31-35, 2010.
- [20] Kil S., Lee J., Shen D., Ryu J., Lee E., Min H., and Hong S., "Lossless Medical Image Compression using Redundancy Analysis," *International Journal of Computer Science and 50 Network Security*, vol. 6, no. 1A, pp. 50-56, 2006.
- [21] Kivijarvia J., Ojala T., Kaukoranta T., Kuba A., Nyulb L., and Nevalainen O., "A Comparison of Lossless Compression Methods for Medical Images," *Computerized Medical Imaging and Graphics*, vol. 22, no. 4, pp 323-39, 1998.
- [22] Koh C. and Mukherjee J., "New Efficient Methods of Image Compression in Digital Cameras with Color Filter Array," *IEEE Transactions on Consumer Electronics*, vol. 49, no. 4, pp. 1448-1456, 2003.
- [23] Lam K., Lau W., and Li Z., "The Effects on Image Classification using Image Compression Technique," available at: http://www.isprs.org/proceedings/XXXIII/congress/part7/744_XXXIII-part7.pdf, last visited 2000.
- [24] Liu D., Sun X., and Wu F., "Edge-Based in Painting and Texture Synthesis for Image Compression," in *Proceedings of IEEE International Conference on Multimedia and Expo*, Beijing, pp. 1443-1446, 2007.
- [25] Palanisamy G. and Samukutti A., "Medical Image Compression using a Novel Embedded Set Partitioning Significant and Zero Block Coding,"

- the International Arab Journal of Information Technology*, vol. 5, no. 2, pp 132-139, 2008.
- [26] Ramesh S. and Shanmugam A., "Medical Image Compression using Wavelet Decomposition for Prediction Method," *International Journal of Computer Science and Information Security*, vol. 7, no. 1, pp. 262-265, 2010.
- [27] Ruchika M. and Singh A., "Compression of Medical Images using Wavelet Transforms," *International Journal of Soft Computing and Engineering*, vol. 2, no. 2, pp. 339-343, 2012.
- [28] Satyanarayana B., Govardhan A., and Murthy H., "A Novel Method of Shape Based Image Compression using Spectral Curvature Scaling," *International Journal of Advanced Engineering and Application*, vol. 1, pp. 203-206, 2010.
- [29] Sousa C., Cavalcante A., Guilhon D., and Barros A., "Image Compression by Redundancy Reduction," in *Proceedings of the 7th International Conference on Independent Component Analysis and Signal Separation*, Springer Berlin Heidelberg, pp. 422-429, 2007.
- [30] Sudha V. and Sudhakar R., "Two Dimensional Medical Image Compression Techniques-A Survey," *ICGST-GVIP Journal*, vol. 11, no. 1, pp. 9-20, 2011.
- [31] Sumalatha R. and Subramanyam M., "Region Based Coding of 3D Magnetic Resonance Images for Telemedicine Applications," *International Journal of Computer Applications*, vol. 5, no.12, pp. 1-3, 2010.
- [32] Tamilarasi M. and Palanisamy V., "An Efficient Embedded Coding For Medical Image Compression using Contourlet Transform," *European Journal of Scientific Research*, vol. 49, no. 3, pp. 442-454, 2011.
- [33] Thakur N. and Kakde O., "Color Image Compression with Modified Fractal Coding on Spiral Architecture," *Journal Of Multimedia*, vol. 2, no. 4, pp. 55-66, 2007.
- [34] Vaquero J., Vilar R., Santos A., and Pozo F., "Cardiac MR Imaging Compression: Comparison between Wavelet Based and JPEG Methods," in *Proceedings of Computers in Cardiology*, Vienna, Austria, pp. 657-660, 1995.
- [35] Vidhya K. and Shenbagadevi S., "A Two Component Medical Image Compression Technique," *International Journal of Recent Trends in Engineering*, vol. 1, no. 1, pp. 591-593, 2009
- [36] Walmsley N., Skodras A., and Curtis K., "A Fast Picture Compression Technique," *IEEE Transactions on Consumer Electronics*, vol. 40, no. 1, pp. 11-19, 2002.
- [37] Wang Z., Bovik A., Sheikh H., and Simoncelli E., "Image Quality Assessment: From Error Visibility to Structural Similarity," *IEEE Transactions on Image Processing*, vol. 13, no. 4, pp. 600-612, 2004.
- [38] Wu F. and Sun X., "Image Compression by Visual Pattern Vector Quantization," in *Proceedings of Data Compression Conference*, Snowbird, pp. 123-131, 2008.
- [39] Yang M., Trifas M., Chen L., Song L., Buenos-Aires D., and Elston J., "Secure Patient Information and Privacy in Medical Imaging," *Journal of Systemics, Cybernetics and Informatics*, vol. 8, no. 3, pp 63-66, 2011.
- [40] Zeybek E. and Nait-Ali A., "Improvement of JPEG2000 Lossy Compression Performances using Preliminary Non-linear Filtering," *International Journal of Information and Communication Engineering*, vol. 4, no. 1, pp. 24-29, 2008.
- [41] Zukoski M., Boulton T., and Iyriboz T., "A novel Approach for Medical Image Compression," *International Journal Bioinformatics Research and Applications*, vol. 2, no. 1, pp. 89-103, 2006.



TMP Rajkumar received his BE degree in electronics engineering from SSIT Tumkur and MTech in industrial electronics from Karnataka Regional Engineering college (currently known as NITK) Surthkal. Presently he is perusing his

PhD from JNTU Hyderabad and working as faculty in E and C Dept Anjuman Engineering College Bhatkal. He is Fellow member of Institution of Engineers (FIE) India, and also Fellow member of Electronics and Telecommunication Engineers (FIETE).



Mrityunjaya Latte received his BE degree in electrical engineering and ME from SDM College of Engineering and Technology. Dharwad, Karnataka India. He was awarded the PhD degree in 2004 for his work in the area of digital Signal

Processing. Presently he is working as Principal, JSS Academy of Technical Education, Bangalore. His research interests include coding, image processing and multiresolution transforms. He received a "Best PAPER" award for his paper in a National Conference NCSSS 2002 held at Coimbatore India MES.